Research Article

Effects of L-dopa and p-coumaric acid combination on oxidative stress, DNA damage, and mitochondrial apoptosis in neuroblastoma cells

Effects of L-dopa and p-coumaric acid combination on oxidative stress, DNA damage, and mitochondrial apoptosis in neuroblastoma cells

Nebiye Pelin Turker[1] and Elvan Bakar[2]

[1]Technology Research Development Application, and Research Center, Trakya University, Edirne, Turkey;
[2]Department of Basic Pharmaceutical Sciences, Faculty of Pharmacy, Trakya University, Edirne, Turkey.

Abstract

This study aimed to investigate the effects of levodopa (L-dopa), p-coumaric acid, and combinations in the neuroblastoma (N1E-115) cell. L-dopa and L-dopa plus p-coumaric acid group caused oxidative stress by increasing 12.5 and 3.7-fold in superoxide dismutase gene, 11.5 and 4.8-fold increase in catalase gene, respectively. In L-dopa and L-dopa plus p-coumaric acid application, p21 gene expression increased 1.3-fold and 3.2-fold, and the cell cycle stopped in the G1 phase in response to stress in the treatment groups. In the application of L-dopa plus p-coumaric acid to N1E-115 cells, the BCL-2 gene, which is an apoptosis inhibitor, was suppressed and the BAX gene increased 13-fold compared to the control. As a result, it was determined that the cytotoxic effect of L-dopa plus p-coumaric acid application was less than the individual application of the substances, and p-coumaric acid had an inhibitory effect on L-dopa-induced stress.

Introduction

Neuroblastoma is a ganglion cell-derived tumor group consisting of primordial neural crest cells (Rha et al., 2003). Through advances in basic science and clinical research in the treatment of neuroblastoma in recent years, new therapeutic options have been sought.

In Parkinson's, Alzheimer's, and neurological cancers, dopaminergic neuron loss is characterized by a significant decrease in the neostriatal ingredient of dopamine and its main metabolites (Hornykiewicz, 1966, 1973, 1988). With the preferred treatment, the administration of L-dopa is aimed at its conversion to dopamine by catalyzing decarboxylase in the brain and thus increasing dopamine in surviving neurons. Although L-dopa can alleviate most of the signs of neurodegenerative diseases, treatment is not sufficient and dopaminergic cells proceed to die in most patients taking L-dopa

therapy (German et al., 1989). Studies have found that L-dopa and dopamine are cytotoxic to cells in culture. The mechanism of dopamine toxicity in melanoma and other tumor cells is not clear yet. Studies show that focusing on the G1/S phase of the cell cycle and inhibition of DNA synthesis in cells is necessary (Oberley and Buettner, 1979; Park et al., 1990). Inhibition of ribonucleotide reductase affects cytotoxicity (Pawelek and Lerner, 1978).

p-Coumaric acid, a phenolic acid of the hydroxycinnamic acid family, is synthesized by phenylalanine and tyrosine (Ossio et al., 2017; Kianmehr et al., 2020). It can be converted into phenolic acids, flavonoids, secondary metabolites, and lignin precursors. A protective role in atherosclerosis, oxidative cardiac injury, oxidative heart damage, UV-ocular tissue damage, neuron damage, anxiety, gout, and diabetes had been published (Kianmehr et al., 2020).

This study aims to elucidate the possible mechanisms by which combined L-dopa plus p-coumaric acid causes neuroblastoma toxicity. The idea is that p-coumaric acid may be associated with oxidative or non-oxidative dopamine toxicity. Therefore, in this study, neuroblastoma (N1E-115) cells were exposed to concentrations of L-dopa and L-dopa plus p-coumaric acid for 24 hours.

Materials and Methods

Cell culture and passage

Neuroblastoma N1E-115 (ATCC® CRL2263™) cell line was used in the study. The cell line was cultured in the flow room [Safe Fast Elite (EN 12469 2000)]. In the passage and culture of cells, DMEM:EMEM:Ham's F-12 (Multicell) (in proportion as: 1:1:1), 1% penicillin-streptomycin (Multicell (450-201-Z2), 1% L-glutamine [Multicell (609-065-E2)], 5% newborn medium containing bovine serum (Multicell, FBS-HI-IIA) was used and incubated in sterile incubators at 37ºC and 5% CO_2 (Panasonic). Cultured cell lines were replicated until the 5th passage and stocks were prepared for further use (DMSO (Merck 67-68-15) was frozen in liquid nitrogen in medium-containing cryotubes and stored at -150°C (Panasonic). In all studies, it started from the 5th passage of the cell lines, and the study was terminated at the 15th passage.

Application of molecules and dose determination

Cell viability and proliferation were determined by an MTT assay. First, L-dopa, p-coumaric acid, and L-dopa plus p-coumaric acid combination doses were calculated and LD_{50} doses was determined.

RNA isolation and cDNA synthesis

Pure Link RNA isolation kit was used for total RNA isolation from the N1E-115 cell line (Invitrogen™-12183018A). The amount of RNA isolated was determined with NanoDrop (NanoQ Optizen). PCR conditions using the cDNA reverse transcription kit (Applied Biosystems-00709629) step 1: 25°C, 10 min; step 2: 37°C, 120 min; step 3: 85°C was programmed to be 5 min and cDNA synthesis were done.

Box 1: MTT Assay

Principle

NAD(P)H-linked oxidoreductase in living cells converts the yellow MTT reagent to dark purple formazan (an insoluble crystal). The darker the fluid, the more live and metabolically active cells there are.

Requirements

Benchtop centrifuge; Dimethyl sulfoxide; Ethanol; Formazan; Incubator with 5% CO_2 at 37°C; Microplates-96 well; Modified Eagle medium culture of Dulbecco (5% FBS); MTT (3-[4,5-dimethylthiazol-2-yl]-2,5 diphenyl tetrazolium bromide); Multi-channel pipette (0.01-0.3); Multiwell plate reader (Thermofisher, Microplate reader); N1E-115 cells; Plate shaker; Round or flat bottom well; Single channel pipette (0.001-1 mL)

Procedure

MTT solution preparation

Step 1: Dissolve 150 mg of MTT powder in 30 mL of phosphate buffer solution

Step 2: In the dark, mix the solution using a magnetic stirrer for roughly 1 hour

Step 3: Sterilize the solution using a 0.22 mm filter and store in 10 mL aliquots at -20°C

Incubation of cell

Day 1

Step 1: Culture N1E-115 cells in 10 mL of Dulbecco's modified Eagle's medium

Step 2: Centrifuge the medium for 2.3 min in a sterile hawk tube (15 mL) at 2500 rpm

Step 3: Drain the medium and resuspend the cells in 1 mL of culture media

Step 4: Count and record cells per mL aseptically

Step 5: Dilute the cells to 10^6 cells/mL. Use Dulbecco's modified Eagle medium to dilute cells

Step 6: Add 180 µL of cells (10^5 cells total) to each well and incubate for 24 hours

Day 2

Step 1: Plant the substances to be applied in the wells at 20 µL

Step 2: Final volume should be 200 µL/well

Step 3: Cells are plated in 8 replicates to minimize variation in results. Incubate cells for 24 hours

Day 3

Step 1: Add 20 µL of 0.5 mg/mL MTT to each well. Everything should be done aseptically

Step 2: Next, incubate the plate for an additional 2-4 hours at 37°C in a CO_2 incubator, depending on the cell. Intracellular formazan crystals wait until it becomes visible under the microscope

Step 3: Remove the medium and add 100-200 µL of DMSO

Step 4: Measure absorbance at 492 nm using the microplate reader

Calculation

IC_{50} values were calculated by probit analysis of SPSS 20 software

Reference

Deivasigamani et al., 2019

Reference (Video)

Bahuguna et al., 2017

Real-Time PCR (qRT-PCR)

Quantstudio 6 Flex qRT-PCR system (Sybr green method (PowerSYBR green- Applied Biosystems-1805575)), which can read 384-well microplates, was used. GAPDH was used as the endogenous gene and samples were analyzed. The genes used and their sequences are given in Supplementary Table I.

Determination of intracellular ion concentration

After the LD_{50} value was determined, the cells were taken into 6-well plates and this LD_{50} value was applied to N1E-115 cell lines. After 24 hours of incubation, the cells of the treatment and control groups were incubated with nitric acid overnight and the amounts of sodium and potassium were determined on the ICP-MS device (Agilent 7700x ICP-MS).

Genetic stability analysis with random amplified polymorphic DNA

The genetic stability of the substances applied in the N1E-115 cell lines was evaluated on the cell by PCR-based RAPD analysis using 3 randomly selected primers [30 OPAF 05 (CCCGATCAGA), 5 OPA 09 (GGGTAACGCC), and 14 OPC 09 (CTCACCGTCC)]. A commercial kit was used for DNA isolation. The quality and quantity of DNA were controlled from the values obtained by running on a 1% agarose gel and also with 260/280 nm UV. The duplicability of PCR amplification was evaluated using chosen primers with isolated DNA samples. RAPD PCR content and the amplification reaction are given in Supplementary Table II.

The PCR products were stained with 2% agarose gel, ethidium bromide (0.5 µg/mL) in 2% tris-acetate EDTA buffer, and were run on electrophoresis and imaged under UV light. The number of bands was registered using the Gel Doc System (Bio-Rad). The size of the amplification products was guessed using the 100–3000 bp DNA ladder (Biomatic, M7123-100 loads). Genomic template stability (GTS (%) was calculated with the following equation:

GTS%=100-(100a/n),

where 'n' is the number of bands detected in control DNA profiles, 'a' is the average number of changes in DNA profiles

Immunofluorescence staining method

N1E-115 cell lines were cultured for 24 hours in the presence of L-dopa, p-coumaric acid, and L-dopa plus p-coumaric acid, and then the cell lines were washed with PBS. Cas3,7 (Thermofisher Cat. No. C10423), and cell viability imaging kit (blue/red) (Thermofisher Cat. No. R37610) using fluorescence microscopy (Carl Zeiss, Axio Observer) by staining according to the kit protocol images were obtained.

Statistical analysis

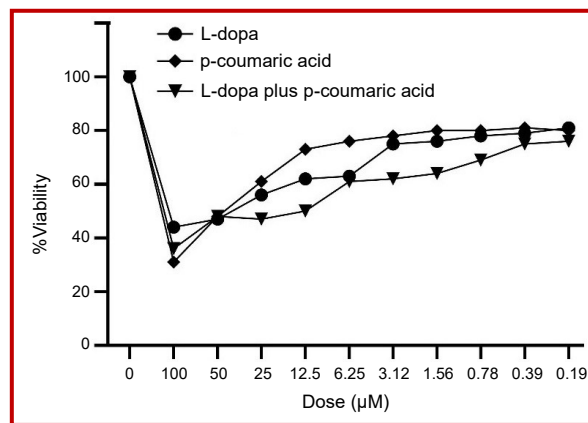In the MTT study, Probit analysis was performed to

Figure 1: MTT cell viability (%) on N1E-115 neuroblastoma cell line after treatment with L-dopa, p-coumaric acid and both

determine the IC_{50}. In the ICP-MS study, one-way of variance (ANOVA) Duncan test was preferred. In real time PCR studies, GADPH gene expression was used as ΔΔCT method and calibration curve and correction factor in determining gene expression differences between groups. In the comparison of control and trial groups, ANOVA test was performed and the groups in which the averages entered were determined by Duncan Test ($p<0.0001$). SPSS 20 (university licensed) were used in all analyzes.

Results

MTT analysis results

Within the scope of the study, the effect of L-dopa and L-dopa plus p-coumaric acid combinations on cell viability for 24 hours in N1E-115 cell lines was determined with the MTT. Exposure of the N1E-115 cell line to L-dopa and L-dopa plus p-coumaric acid for 24 hours caused dose-related death on cell viability. The LD_{50} dose, which was 52.5 µM and 25.4 µM with the application of L-dopa and p-coumaric acid alone, 7.6 µM was found in the combination application. The cell viability (%) graph obtained from MTT results is given in Figure 1. ANOVA test revealed that there was a statistically significant difference in mean values between at three groups (F(17.1), 95% C.I., $p=0.01$).

Gene expression results by qRT-PCR

In the study, changes in gene expressions were determined by the qRT-PCR method using cDNAs obtained from RNAs isolated from neuroblastoma cell lines. The changes in the expressions of the genes determined in the N1E-115 neuroblastoma cells of the groups in which the applications were made compared to the control group were included in the study as 3 repetitions and statistical evaluations were made.

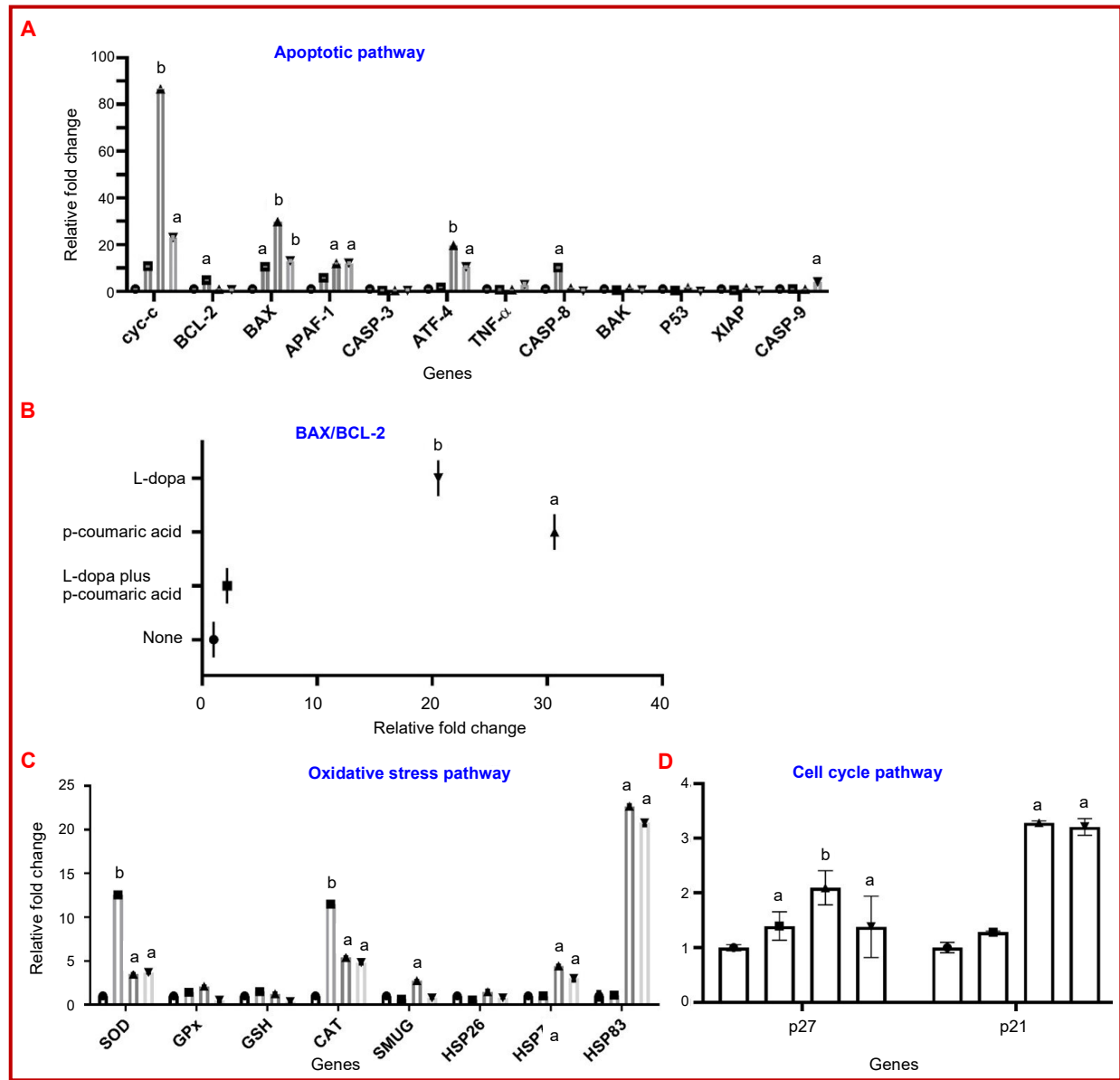The changes caused by the combinations of L-dopa and L-dopa plus p-coumaric acid in the expression of

Figure 2: On N1E-115 neuroblastoma cell line, mRNA expression of apoptotic signaling pathway genes (n=3 ± SD) (relative to the control group; one-way ANOVA post hoc Duncan, [a,b]p<0.05)[A]. BAX/BCL-2 ratio relative fold change (n=3 ± SD) (relative to the control group; one-way ANOVA post hoc Duncan, [a,b]p<0.05)[B]. mRNA expression of oxidative stress signaling pathway genes (n=3 ± SD) (relative to the control group; one-way ANOVA post hoc Duncan, [a,b]p<0.05)[C]. mRNA expression of cell cycle signaling pathway genes (n=3 ± SD) (relative to the control group; one-way ANOVA post hoc Duncan, [a,b]p<0.05)[D]

apoptotic signaling pathway (intrinsic and extrinsic apoptosis) genes are given in Figure 2A. When the L-dopa plus p-coumaric acid combination was applied to neuroblastoma cells, it was determined that the BCL-2 gene, which is an apoptosis inhibitor, was suppressed and the BAX gene increased 13.0 ± 0.5 times compared to the control (Figure 2A). There was a statistically significant difference in BAX gene between at L-dopa plus p-coumaric acid combination (F:5600.42, p=0.01, 95% C.I. = [13.04]). This increase in BAX expression level disrupted the mitochondrial membrane and initiated apoptosis by releasing cytochrome-c into the

cytosol. The increase in BAX expression level in L-dopa administration could not suppress the activity of BCL-2 but increased BAX gene expression changed the BAX/BCL-2 ratio (Figure 2B). One-way ANOVA was performed to compare the effect of gene expressions on three different groups. There was a statistically significant difference in the mean of some apoptosis genes between groups (p<0.05). Average relative fold changes and standard deviation values are given in Table I.

Figure 2C shows the changes in the expression of genes linked to the oxidative stress pathway induced by
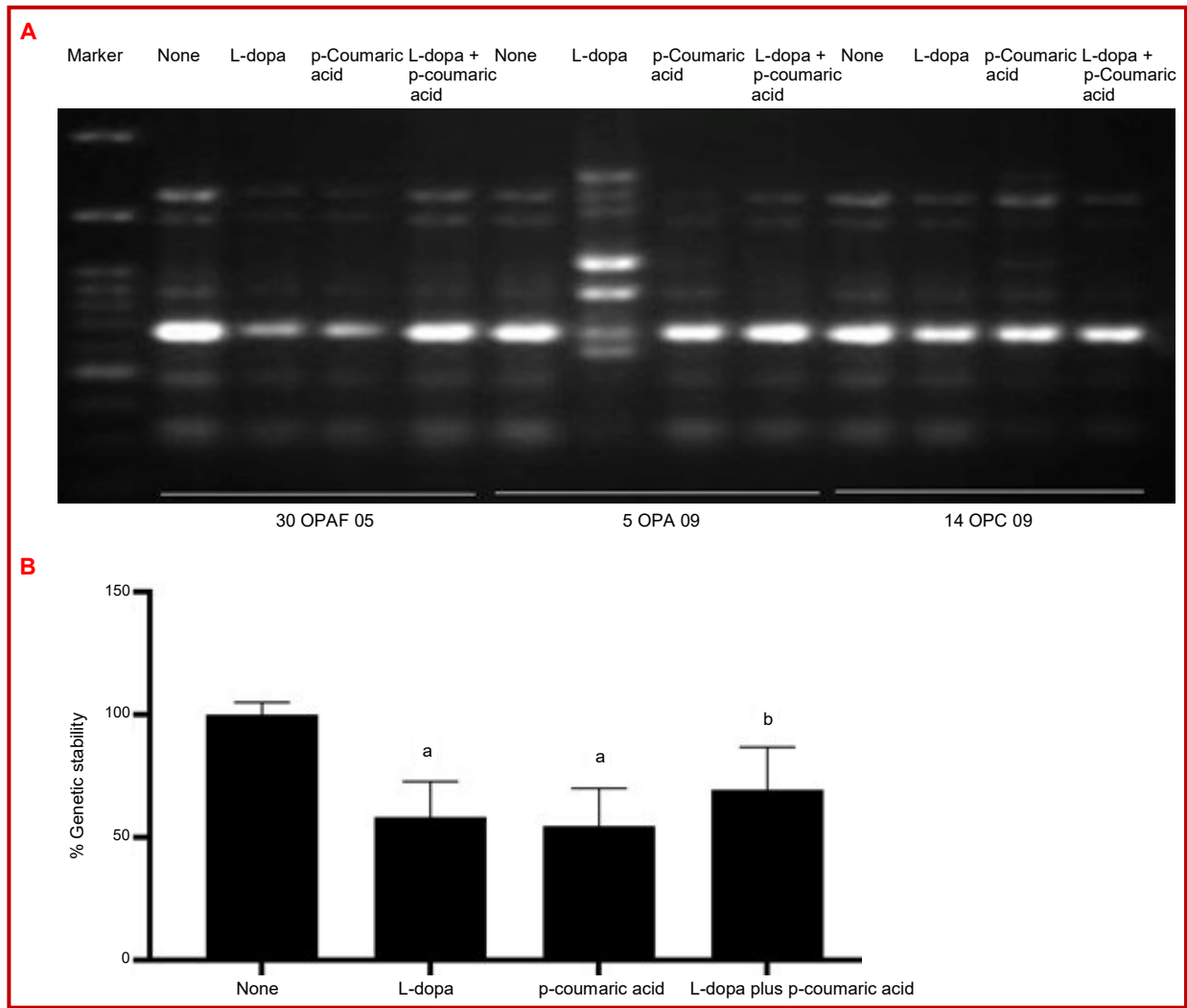
Figure 3: On N1E-115 neuroblastoma cell line, Agarose gel electrophoresis image (n_{primer}: 3, Marker: 100 bp)[A]. Genetic stability analysis with RAPD PCR (n_{primer}: 3, ± SD). (relative to the control group; one-way ANOVA post hoc Duncan, [a,b]$p<0.05$)[B]

combinations of L-dopa and L-dopa + p-coumaric acid. A one-way ANOVA was performed to compare the effect of three groups' oxidative stress genes (95% C.I.). Application of L-dopa, L-dopa plus p-coumaric acid combinations caused oxidative stress in N1E-115 cells and it was determined that it caused oxidative stress by increasing 12.5 ± 0.1 fold, 3.7 ± 0.1 fold in superoxide dismutase gene, 11.5 ± 0.1 fold, and 4.8 ± 0.0 fold in catalase gene, respectively ($p<0.05$). There was no statistically significant difference in glutathione peroxidase ($p=0.101$) and reduced glutathione ($p=0.055$). Average relative fold changes and standard deviation values are given in Table I.

Changes in p21cip1 and p27kip1 gene expressions are given in Figure 2D. A one-way ANOVA revealed that there was a statistically significant difference between groups. There was no statistically significant difference in p21 genes between groups (F:187.74, 95% C.I., $p=0.066$). According to the results of the analysis, the

p21[cip1] gene expression in the N1E-115 cell lines was increased by 1.4 ± 0.3 and 1.3 ± 0.5 fold, respectively, in the application of L-dopa and L-dopa plus p-coumaric acid combinations compared to control. The highest increase in p27[kip1] gene expression was observed in L-dopa plus p-coumaric acid (3.2 ± 0.3) (p27, F: 16.346, 95% C.I., $p=0.01$). Average relative fold changes and standard deviation values are given in Table I.

Results of intracellular Na^{+}, K^{+} determination

L-dopa, L-dopa plus p-coumaric acid administration disrupted the intracellular ion balance (Na^{+}, K^{+}) (data are not shown). While there was a 1.6-fold increase in ions with L-dopa application, there was a 2.4-fold decrease in L-dopa plus p-coumaric acid application (one-way ANOVA post hoc Duncan, $p<0.05$).

Genetic stability analysis results by RAPD PCR

Fingerprint profiles of cells made by RAPD markers were evaluated to confirm whether the cells were
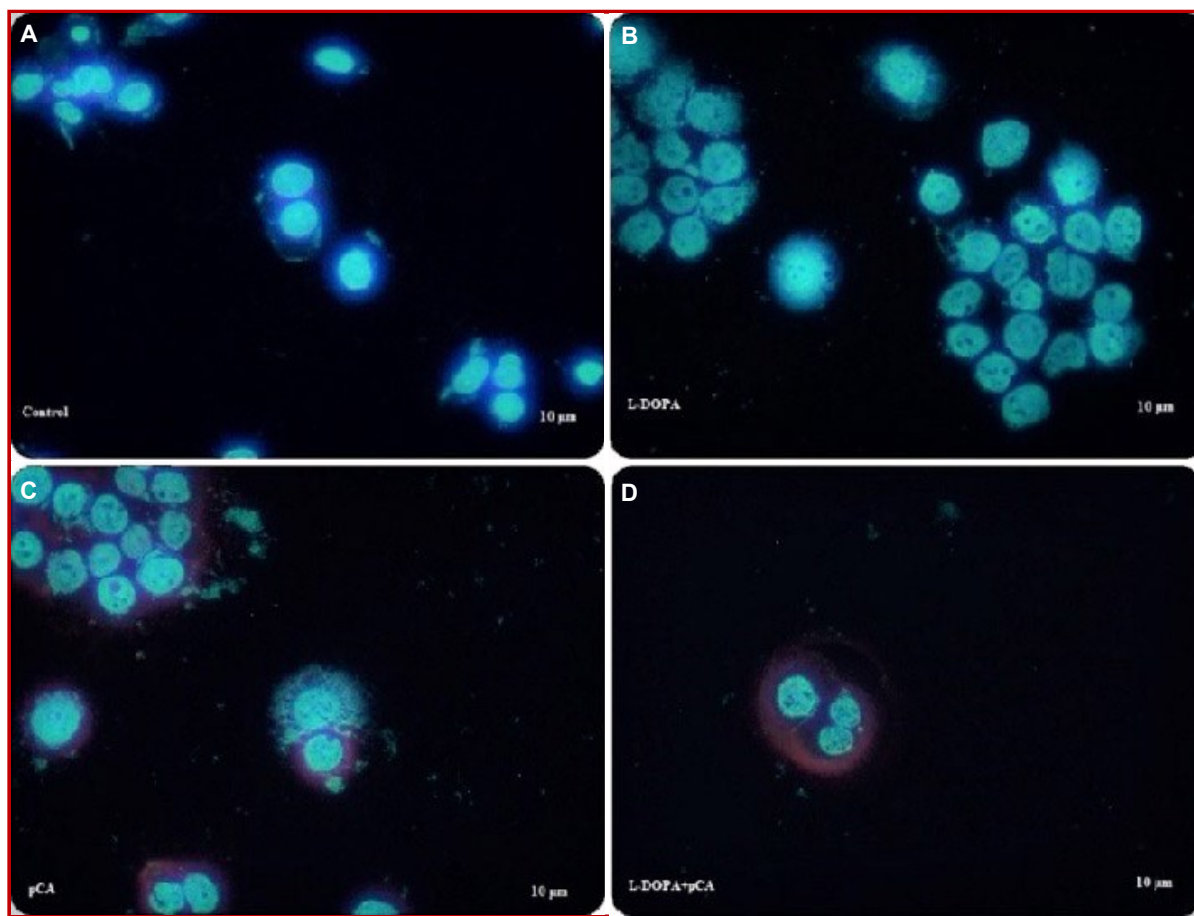
Figure 4: Immunofluorescent staining of control (A), l-dopa (B), p-coumaric acid (C), L-dopa plus p-coumaric acid (D) groups of neuroblastoma (N1E-115) cells by cell viability imaging kit caspase 3/7. (Blue: live cell; Red: dead cell; Green: caspase 3/7 positive)

genetically stable with the substances applied in cell culture applications. A total of 3 random RAPD primers were tested for initial screening (Gel image Figure 4). For each RAPD primer, the treatment groups were compared with the control group, and the genetic stability ratios were calculated by determining the number of bands that disappeared (Figure 3). A significant difference was found in the combination of L-dopa plus p-coumaric acid compared to one-way ANOVA (p=0.02).

Immunofluorescence staining results

The images of cas3,7 and cell viability (blue/red) staining analysis performed in the N1E-115 neuroblastoma cell line are given in Figure 4. In the staining results, the dead cell density was highest in the L-dopa application compared to the control. In the L-dopa plus p-coumaric acid application, as expressed in the qRT-PCR results, the change of BAX/BCL-2 ratio and the initiation of cytochrome-c release was confirmed by apoptotic cells.

Discussion

The combination group formed a more stable genetic

structure in N1E-115 cells compared to L-dopa or p-coumaric acid applied alone. L-dopa induced oxidative stress-induced cellular death. In addition, the combination application caused an increase in TNF-α gene expression by binding TNF-α, one of the death signals, to the Fas/TNFR/DR5 death receptors on the cell surface. With the increase in TNF-α, CAS-9 was activated and there was an increase in gene expression compared to the control. In combination application, it is seen that the increases in the HSP70 and HSP83 genes show that p-coumaric acid has a protective effect against the oxidative stress caused by L-dopa in neuroblastoma cells. In addition, especially in the application of L-dopa plus p-coumaric acid combination increased ATF-4 gene expression. It is thought that stress-sensitive genes may be increased as the main transcription factor in response to eIF-2-alpha/EIF2S1 phosphorylation caused by L-dopa-induced oxidative stress and to promote cell recovery. In the results of intracellular ion analysis with ICP-MS. With the application of L-dopa, it is confirmed that sodium and potassium ions, which increase 1.6 times compared to the control, increase the ion permeability of the cell due to oxidative stress. In L-dopa and p-coumaric acid combination (2.4 fold) administration, a decrease in sodium and potassium

Table I

Statistically significant apoptotic signal path, oxidative stress singal path and cell cycle control genes

Genes	Relative fold change		
	L-dopa	p-Coumaric acid	L-dopa plus p-coumaric acid
Apoptotic signal path			
cyc-c	10.8 ± 0.2↑	86.6 ± 0.2↑	23.0 ± 0.0↑
BAX	10.6 ± 0.3↑	29.9 ± 0.1↑	13.0 ± 0.5↑
BCL-2	4.9 ± 0.1↑	1.0 ± 0.4↓	0.6 ± 0.0↓
APAF-1	5.9 ± 0.1↑	12.0 ± 1.1↑	12.1 ± 0.0↑
ATF4	1.6 ± 0.1↑	19.7 ± 1.2↑	10.4 ± 0.0↑
CASP-9	1.1 ± 0.0↑	1.0 ± 0.1↓	4.0 ± 0.0↑
Oxidative stress signal path			
Superoxide dismutase	12.5 ± 0.0↑	3.5 ± 0.0↑	3.7 ± 0.1↑
Catalase	11.5 ± 0.1↑	5.4 ± 0.4↑	4.8 ± 0.0↑
Cell cycle control			
p21^{cip1}	1.4 ± 0.3↑	2.1 ± 0.2↑	1.3 ± 0.5↑
p27^{kip1}	1.3 ± 0.4↑	3.3 ± 0.2↑	3.2 ± 0.36↑

channels occurred compared to the control. Results of intracellular ion analysis by qRT-PCR confirm that death caused by L-dopa plus p-coumaric acid combination application is caused by apoptosis.

Auto-oxidation of L-dopa can occur both extracellularly and intracellularly, whereas cells do not have a dopamine transport system, and therefore dopamine likely only causes extracellular damage (Leanza et al., 2013). This study suggests that L-dopa is a toxic agent. Alie et al. (1995), in their study on L-dopa toxicity in PC12 cells, carbidopa, an inhibitor of A-aromatic L-amino acid decarboxylase, is caused by dopamine composed of exogenously added L-dopa of L-dopa cytotoxicity. They investigated that it does not originate. The results showed that L-dopa is toxic to PC12 cells through its auto-oxidation (Basma et al., 1995). Pedrosa R. et al. (2002) conducted a study to evaluate the neurotoxicity of L-dopa and dopamine and oxidative stress/apoptosis.

This study was made to appreciate the importance of dopamine and L-dopa in neuronal cell death. The results showed that besides H_2O_2 production and quinone generation, L-dopa- and dopamine-dependent cell death may result from apoptosis induction by an increase in caspase3 activity. Caspase-3 activity, which increased with dopamine administration, also showed dopamine-induced toxicity by a mechanism distended of oxidative stress (Pedrosa and Soares-da-Silva, 2002). In this study, the increased catalase gene expression with L-dopa administration indicates that hydrogen peroxide is formed during the auto-oxidation of L-dopa. The anti-proliferative effect of p-coumaric acid on glioblastoma cell lines (A172, LN-229, LN-18, and LBC3) were evaluated (Naumowicz et al., 2019). Concentrations of 0.5–10 mmol/dm³ for all four cell lines evaluated were found to cause reductions in cell

viability. However, the cytotoxic effect of p-coumaric acid was found to be most effective in A172 and LBC3 cells. A significant increase in CASP-9 activity was sighted in A172 cells applied to p-coumaric acid. Administration of 5 mmol/dm³ p-coumaric acid produced a significant increase in CASP-9 activity in LBC3 cells, while a concentration of 8 mmol/dm³ did not significantly increase this activity. Similarly, in A172 cells, they observed an almost two-fold increase in caspase 3/7 activity at both p-coumaric acid doses tested. Caspase 3/7 activity was reduced in LBC3 cells at both 5 and 8 mmol/dm³ p-coumaric acid doses. This effect showed that events other than apoptotic cell death may be responsible (Naumowicz et al., 2019). Xiuci Yan et al. (2020); studied the protective effect of p-coumaric acid to alleviate hepatocyte damage induced by palmitic acid. In this study, intracellular lipid accumulation decreased and the percentage of viability increased with the progression of fatty acid p-oxidation and lipolysis in PA-treated hepatocytes. They concluded that p-coumaric acid is effective on multiple hepatocellular metabolic lanes to arrange lipid metabolism. They reported that their results increased the likelihood that the therapeutic use of p-coumaric acid could alleviate hepatic lipid metabolic disorders (Yan et al., 2020). Human cancer cell lines such as colon (HT29-D4, HCT-15), glioblastoma, lung (A549), and neuroblastoma have demonstrated anti-cancer activity with decreased proliferation and reduced adhesion-suppressed cell migration (Chien et al., 1999; Javadov et al., 2011). Caffeic acid, tyrosol and p-coumaric acid are potent inhibitors of 5-S-cysteinyl-dopamine induced neurotoxicity (David et al., 2010). It was determined that p-coumaric acid is a dopamine inhibitor (Vauzour et al., 2010). Various channels act a role in ion balance in organelles such as the endoplasmic reticulum, lysosome, nucleus, and mitochondria. In mitochondria, which plays a

centrical role in apoptosis, the transition of ion channels can cause the death of cancer cells. In oncotherapy, it is very important to selectively stimulate the inner mitochondrial membrane permeability of cancer cells. Certain cellular stresses and cytotoxic agents stimulate a prime example of such a pathway that is considered to be the last common pathway of cell death, namely the mitochondrial transmissivity transition (Brenner and Grimm, 2006; Brenner and Moulin, 2012). Opening large calcium to mitochondrial transmissivity transition makes the inner mitochondrial membrane permeable to ions, activated by oxidative stress. The mitochondrial membrane potential is hoped to attend in the regulation of ROS production. The expression of the mitochondria-targeted potassium channel (Kv1.3) structure, which plays a significant role in the potassium channel, has been defined as a target of the Bax gene, indicating the physical interplay between the proteins in apoptotic cells. Incubation of Kv1.3 positive isolated mitochondria with BAX has been found to stimulate apoptosis, including ROS production, membrane potential changes, and cytochrome c release (Szabo et al., 2008; Szabo et al., 2011). The loss of mitochondrial membrane potential, ie, decrease in ions, induced apoptosis associated with cytochrome c release and caspase activation (Fernandez-Salas et al., 2002).

Conclusion

p-Coumaric acid causes death in N1E-115 cell lines due to apoptosis. Addition of L-dopa indicates that alternative therapies are of great importance in the treatment of diseases.

Financial Support

Ethical Issue

The development, acquisition, authentication, cryopreservation, and transfer of cell lines between laboratories were followed according to the guidelines published in British Journal of Cancer, 2014

Conflict of Interest

Authors declare no conflict of interest

Acknowledgement

References

Adamczyk B, Tharmalingam T, Rudd PM. Glycans as cancer biomarkers. Biochim Biophys Acta. 2012; 1820: 47-53.

Anden NE, Hfuxe K, Hamberger B, Hokfelt T. A quantitative study on the nigro-neostriatal dopamine neuron system in the rat. Acta Physiol Scand. 1966; 67: 106-12.

Annis MG, Soucie EL, Dlugosz PJ, Cruz-Aguado JA, Penn LZ, Leber B, Andrews DW. Bax forms multispanning monomers that oligomerize to permeabilize membranes during apoptosis. EMBO J. 2005; 24: 2096-03.

Bahuguna A, Khan I, Bajpai VK, Kang SC. MTT assay to evaluate the cytotoxic potential of a drug. Bangladesh J Pharmacol. 2017; 12: 115-18.

Basma AN, Morris EJ, Nicklas WJ, Geller HM. L-dopa cytotoxicity to PC12 cells in culture is via its autoxidation. J Neurochem. 1995; 64: 825-32.

Blunt SB, Jenner P, Marsden CD. Suppressive effect of L-dopa on dopamine cells remaining in the ventral tegmental area of rats previously exposed to the neurotoxin 6-hydroxydopamine. Mov Disord. 1993; 8: 29-33.

Brenner C, Grimm S. The permeability transition pore complex in cancer cell death. Oncogene 2006; 25: 744-56.

Brenner C, Moulin M. Physiological roles of the permeability transition pore. Circ Res. 2012; 111:237-47.

Chien MM, Zahradka KE, Newell MK, Freed JH. Fas-induced B cell apoptosis requires an increase in free cytosolic magnesium as an early event. J Biol Chem. 1999; 274:059-66.

Cohen G. Monoamine oxidase and oxidative stress at dopaminergic synapses. J Neural Transm Suppl. 1990; 32: 29-38.

Cohen G. Monoamine oxidase, hydrogen peroxide, and Parkinson's disease. Adv Neurol. 1987; 45: 19-25.

Cohen G. The pathobiology of Parkinson's disease: Biochemical aspects of dopamine neuron senescence. J Neural Transm Suppl. 1983; 19: 89-03.

Fernández-Salas E, Suh KS, Speransky VV, Bowers WL, Levy JM, Adams T, Pathak KR, Edwards LE, Hayes DD, Cheng C, Steven AC. mtCLIC/CLIC4, an organellular chloride channel protein, is increased by DNA damage and participates in the apoptotic response to p53. Mol Cell Biol. 2002; 22: 610-20.

German DC, Manaye K, Smith WK, Woodward DJ, Saper CB. Midbrain dopaminergic cell loss in Parkinson's disease: Computer visualization. Ann Neurol. 1989; 26: 107-14.

Hornykiewicz O. Dopamine (3-hydroxytyramine) and brain function. Pharmacol Rev. 1966; 18: 25-64.

Hornykiewicz O. Neurochemical pathology and the etiology of Parkinson's disease: Basic facts and hypothetical possibilities. Mt Sinai J Med. 1988; 55: 11-20.

Hornykiewicz O. Parkinson's disease: From brain homogenate to treatment. Fed Proc. 1973; 32: 83-90.

Javadov S, Hunter JC, Barreto-Torres G, Parodi-Rullan R. Targeting the mitochondrial permeability transition: Cardiac ischemia-reperfusion versus carcinogenesis. Cell Physiol

Biochem. 2011; 27: 179-90.

Kianmehr Z, Khorsandi K, Mohammadi M, Hosseinzadeh R. Low-level laser irradiation potentiates anticancer activity of p-coumaric acid against human malignant melanoma cells. Melanoma Res. 2020; 30: 36-46.

Kushner BH. Neuroblastoma: A disease requiring a multitude of imaging studies. J Nucl Med. 2004; 45: 72-88.

Leanza L, Biasutto L, Manago A, Gulbins E, Zoratti M, Szabo I. Intracellular ion channels and cancer. Front Physiol. 2013; 4: 227.

Lonergan GJ, Schwab CM, Suarez ES, Carlson CL. Neuroblastoma, ganglioneuroblastoma, and ganglioneuroma: Radiologic-pathologic correlation. Radiographics 2002; 22: 11-34.

Naumowicz M, Kusaczuk M, Kruszewski MA, Gal M, Krętowski R, Cechowska-Pasko M, Kotyńska J. The modulating effect of lipid bilayer/p-coumaric acid interactions on electrical properties of model lipid membranes and human glioblastoma cells. Bioorg Chem. 2019; 92: 103-42.

Oberley LW, Buettner GR. Role of superoxide dismutase in cancer: A review. Cancer Res. 1979; 39: 41-49.

Ogawa N, Edamatsu R, Mizukawa K, Asanuma M, Kohno M, Mori A. Degeneration of dopaminergic neurons and free radicals. Possible participation of levodopa. Adv Neurol. 1993; 60: 42-50.

Ossio R, Roldan-Marin R, Martinez-Said H, Adams DJ, Robles-Espinoza CD. Melanoma: A global perspective. Nat Rev Cancer. 2017; 17: 93-04.

Park JG, Frucht H, LaRocca RV, Bliss Jr DP, Kurita Y, Chen TR, Henslee JG, Trepel JB, Jensen RT, Johnson BE, Bang YJ. Characteristics of cell lines established from human gastric carcinoma. Cancer Res. 1990; 50: 73-80.

Pawelek JM, Lerner AB. 5,6-Dihydroxyindole is a melanin precursor showing potent cytotoxicity. Nature 1978; 276: 26-28.

Pedrosa R, Soares-da-Silva P. Oxidative and non-oxidative mechanisms of neuronal cell death and apoptosis by L-3,4-dihydroxyphenylalanine (L-DOPA) and dopamine. Br J Pharmacol. 2002; 137: 305-13.

Rha SE, Byun JY, Jung SE, Chun HJ, Lee HG, Lee JM. Neurogenic tumors in the abdomen: Tumor types and ima-ging characteristics. Radiographics 2003; 23: 29-43.

Szabó I, Bock J, Grassmé H, Soddemann M, Wilker B, Lang F, Zoratti M, Gulbins E. Mitochondrial potassium channel Kv1.3 mediates Bax-induced apoptosis in lymphocytes. Proc Natl Acad Sci USA. 2008; 105: 861-66.

Szabo I, Soddemann M, Leanza L, Zoratti M, Gulbins E. Single-point mutations of a lysine residue change function of Bax and Bcl-xL expressed in Bax- and Bak-less mouse embryonic fibroblasts: novel insights into the molecular mechanisms of Bax-induced apoptosis. Cell Death Differ. 2011; 18: 427-38.

Vauzour D, Corona G, Spencer JP. Caffeic acid, tyrosol and p-coumaric acid are potent inhibitors of 5-S-cysteinyl-dopamine induced neurotoxicity. Arch Biochem Biophys. 2010; 501: 106-11.

Yan X, Chen X, Xu X, Liu J, Fu C, Zhao D, Zhao W, Ma R, Sun L. Mechanism underlying p-coumaric acid alleviation of lipid accumula-tion in palmitic acid-treated human hepatoma cells. J Agric Food Chem. 2020; 68: 742-49.

Zoratti M, De Marchi U, Gulbins E, Szabo I. Novel channels of the inner mitochondrial membrane. Biochim Biophys Acta. 2009; 1787: 351-63.

Author Info
Nebiye Pelin Turker (Principal contact)
e-mail: npelinturker@trakya.edu.tr